Long-term moxifloxacin release from a chitosan-based antibacterial coating on polyethylene for biomedical applications

Helton J. Wiggers, [ID] *[a] Nathália F. Sczesny, [ID] [ab] Pascale Chevallier, [ID] [b] Claudia M. da Silva, [ID] [a] Cecilia Z. Bueno, [ID] [a] Francesco Copes [ID] [b] and Diego Mantovani [ID] *[ab]

Medical-grade polyethylene (PE) surfaces are highly susceptible to bacterial colonization and biofilm formation, leading to hospital-associated infections (HAIs). Antibacterial coatings based on natural polymers offer a promising strategy to prevent biofilm establishment while mitigating systemic antibiotic use. However, there are some bottlenecks such as the limited duration of antimicrobial activity and the poor adhesion of the coating to the substrate. In this study, an antibacterial coating with prolonged activity was developed, based on prior work with moxifloxacin-loaded chitosan films. To promote coating adhesion, an approach consisting in wet-chemistry functionalization was studied. PE was treated with piranha solution followed by polydopamine deposition and coated with the moxifloxacin-loaded chitosan formulation. The coatings exhibited uniform coverage; piranha treatment increased roughness and enhanced hydrophilicity, allowing polymer deposition. XPS confirmed successful carbon oxidate species after piranha treatment, and enabled the identification of polydopamine and chitosan, observed by oxygen and nitrogen enrichment. Coating adhesion strength remained stable over 35 days in PBS. Antibiotic release profiles of film and coating were similar, displaying an initial burst (first 10 days) followed by sustained release of moxifloxacin. Antibacterial assay confirmed activity of the coating against *S. aureus* and *E. coli* for up to 160 days. Therefore, a wet-chemistry functionalization approach followed by polydopamine activation yields a strongly adhered antibacterial chitosan-based coating on PE that provides long-term moxifloxacin release and effective inhibition of clinically relevant pathogens. This proof-of-concept study represents a straightforward strategy to produce antimicrobial coatings with prolonged activity to reduce HAIs in medical devices.

1 Introduction

Coatings for implantable medical devices can enhance the safety, functionality, and longevity.[1] A number of surface treatments have been investigated to improve biocompatibility, reduce the risk of infection, prevent adverse immune responses, and promote tissue integration.[2] By tailoring hydrophilicity, roughness, or chemical composition, coatings can also serve as delivery systems for therapeutic agents, including antibiotics or anti-inflammatory drugs.[3] With advances in medical technology, the development of innovative coating materials remains a key focus for addressing persistent challenges such as Healthcare-Associated Infections (HAIs). HAIs represent a critical global public health concern, significantly contributing to increased morbidity, mortality, and economic burden. In western industrialized nations, the prevalence of HAI ranges from 4% to 10%, with a maximum escalation to 30% in intensive care units, constituting the sixth leading cause of death on a global scale.[4] Although advancements in hygiene and hospital protocols have been made, contemporary preventive measures remain insufficient, particularly in managing device-associated infections.

Polyethylene (PE) has been a common material for biomedical applications since the 1960s and remains the most widely used plastic worldwide due to its versatility, durability, and low cost.[5] There are different PE classifications according to its density, with a variety of biomedical applications in the medical field.[6,7] Low-density polyethylene (LDPE) became the material of choice for a wide variety of blood-contacting devices such as cardiac assisting devices, artificial organs, heart valves, intravenous bags, *etc.*[8] However, this polymer is often susceptible to contamination by bacteria, leading to biofilm formation and infections. Biofilms are structured communities of microbial cells embedded in a self-produced extracellular polymeric

[a]Laboratory for Biomaterials and Bioengineering (LBB-BPK), Associação de Ensino, Pesquisa e Extensão BIOPARK, Toledo 85919-899, PR, Brazil. E-mail: helton. wiggers@bpkedu.com.br

[b]Laboratory for Biomaterials and Bioengineering (LBB-UL), Canada Research Chair Tier I, Department of Min-Met-Materials Engineering, Division of Regenerative Medicine of CHU de Quebec Research Center, Laval University, Quebec City, QC G1V 0A6, Canada. E-mail: diego.mantovani@gmn.ulaval.ca

matrix, which strongly protects them against antimicrobial agents and the host immune response.[9]

A common strategy for infection control involves the oral administration of antibiotics. This approach, while convenient and systemic, is sometimes insufficient to achieve enough concentrations at the device surface, where biofilms form. This limitation restricts its efficacy in preventing or eradicating such infections.[10] An alternative approach involves the use of anti-bacterial coatings to prevent the formation of biofilms directly on device surfaces. These coatings can incorporate antibiotics, metallic nanoparticles (*e.g.*, silver, copper), or antimicrobial polymers such as chitosan, offering localized antimicrobial action as a replacement to systemic therapy or in a synergistic manner.[11] Localized delivery has the potential to prevent bi-ofilm formation more effectively than systemic antibiotic administration.[12] Some coatings also enable controlled or stimulus-responsive release, enhancing their clinical potential.[13]

In this context, several strategies have been explored to develop antibacterial surfaces for PE, such as treating PE surfaces with cold plasma to graft antibacterial agents triclosan and chlorhexidine,[14] or incorporating silver or copper into diamond-like carbon coatings,[15] other example is the iso-eugenol coating that prevents colonization of different bacteria.[16] Most of the studies focus on the antibacterial activity upon initial surface contact, this work explores a less studied aspect, the long-term antibacterial performance for LDPE coating.

Among the materials used for antibacterial coatings, chito-san emerges as a versatile film-forming polymer, with tunable physicochemical properties *via* crosslinking and suitability for loading antibiotics, enabling controlled antibiotic release.[17,18] Although chitosan has intrinsic antimicrobial properties, its efficacy can be enhanced by the incorporation of active agents, thereby increasing their local concentration at the device surface. In this context, Sczesny *et al.* (2024) reported a comparative study on the antibacterial activity of chitosan films incorporating different antibiotics, identifying a film formulation with sustained antibacterial activity up to six months due to controlled release of moxifloxacin.[19] These findings motivate the applications of the film as an antibacterial coating onto LDPE substrates, to overcome the challenge of long-term device-associated infections.

LDPE was chemically treated to insert functional groups to allow the adhesion of the chitosan matrix. Additionally, poly-dopamine was deposited on the surface after the chemical treatment to enhance the coating adherence.[20] The coated substrates were characterized in terms of morphology, chemical composition, wettability and adhesion strength. In addition, the release kinetics of moxifloxacin was evaluated and compared with the antibacterial efficacy to assess the potential application for long-term medical devices. This study provides a proof-of-concept for the development of an antibacterial coating on PE, based on a chitosan matrix crosslinked with tannic acid and iron, designed for the controlled release of moxifloxacin.

2 Materials and methods

2.1 Materials

Chitosan (Sigma-Aldrich, medium molecular weight, Shanghai, China) characterized as previously described,[21] low-density polyethylene (LDPE) (GoodFellow, Huntingdon, UK), tannic acid (ACS reagent, Sigma-Aldrich, Beijin, China), phosphate-buffered saline (PBS) (Sigma-Aldrich, Gillingham, UK), iron sulphate heptahydrate (>99%, Êxodo Científica, Sumaré, Bra-zil), moxifloxacin hydrochloride (>99.9%, Prati Donaduzzi, Toledo, Brazil), ethanol (>99.5%, Synth, Diadema, Brazil), acetic acid (99.7%, Synth, Diadema, Brazil), Mueller–Hinton broth (Difco, Sparks, NV, USA), Mueller–Hinton agar (Kasvi, Madrid, Spain), methanol (>99.8%, Biograde, Anápolis, Brazil), tetra-butylammonium sulfate (98%, Êxodo Científica, Sumaré, Bra-zil), phosphoric acid (>98%, Êxodo Científica, Sumaré, Brazil), monobasic potassium phosphate (99%, Dinâmica, Indaiatuba, Brazil), sulfuric acid (98%, Química Moderna, São Paulo, Bra-zil), hydrogen peroxide (30 vol. Êxodo Científica, Sumaré, Bra-zil), dopamine (>98%, Sigma-Aldrich, Darmstadt,Germany), Tris buffer (>99.8%, Sigma-Aldrich, St. Louis, MO, USA), *Escherichia coli* ATCC 8739 (Lab-Elite™, St. Cloud, USA), *Enterococcus faecalis* ATCC 29212 (Lab-Elite™, St Cloud, USA), *Staphylococcus aureus* ATCC 6538 (Lab-Elite™, St Cloud, USA), *Staphylococcus epidermidis* ATCC 12228 (Lab-Elite™, St Cloud, USA), *Pseudomonas aeruginosa* ATCC 9027 (Lab-Elite™, St Cloud, USA), *Salmonella typhimurium* ATCC 14028 (Biomedh, Belo Horizonte, Brazil), *Klebsiella pneumoniae* ATCC 10031 (Lab-Elite™, St Cloud, USA), and a methicillin-resistant *Staphylo-coccus aureus* (MRSA) isolate kindly donated by the Federal University of Paraná, Palotina campus, were used in this study. Dulbecco's modified Eagle's medium (DMEM) (Gibco, Invi-trogen Corporation, Burlington, ON, Canada), resazurin sodium salt (Sigma-Aldrich, Oakville, ON, Canada), human dermal fibroblasts C0045C (Gibco, Invitrogen, Burlington, ON, Canada), fetal bovine serum (FBS) (Gibco, Invitrogen Corpora-tion, Burlington, ON, Canada), trypsin (Gibco, Invitrogen Corporation, Burlington, ON, Canada), penicillin (Gibco, Invi-trogen Corporation, Burlington, ON, Canada) and streptomycin (Gibco, Invitrogen Corporation, Burlington, ON, Canada) were used in this work. All reagents were used as received.

2.2 Film and coating preparation procedure

The film was prepared following a previously described method.[19] Briefly, chitosan was dissolved at 1.5% w/v in 1% v/v acetic acid. The crosslinkers were dissolved in ultrapure water: 50 mg per mL tannic acid (TA) and 3 mg per mL $FeSO_4$ (Fe). A 5 mg per mL moxifloxacin solution was also prepared in ultra-pure water. Firstly, 1.67 mL of Fe, 0.40 mL of TA, and 1.0 mL of the antibiotic were added to 6.67 mL of chitosan solution. The total volume was adjusted to 10 mL by adding ultrapure water. The final mixture contained 20% TA, 5% $FeSO_4$, and 5% of antibiotic relative to the chitosan mass (100 mg). This mixture was stirred magnetically at 1500 rpm to achieve a homogeneous chitosan-based suspension. Afterwards, 10 mL of the mixture

was placed in a 9 cm diameter Petri dish and dried at 37 °C in an oven, forming films with a 20 μm thickness.

The coating was prepared using low-density polyethylene (acronym PE in this text) pieces (1.5 cm × 1.5 cm), which were cleaned by double washing with ethanol for 10 minutes, followed by ultrapure water in an ultrasonic bath (160 W, model SSBu-10L, SolidSteel, Piracicaba, Brazil), also for 10 min. The samples were dried in an oven (model Q317M-32, Quimis, Diadema, Brazil) at 40 °C. The chemical treatment of PE was performed using piranha solution (3 : 1 v/v $H_2SO_4 : H_2O_2$) for 6 hours, followed by thorough rinsing with ultrapure water. The samples were then immersed in a 2 mg per mL dopamine (DOPA) solution dissolved in a 10 mM Tris buffer (pH 8.5). The system was stirred for 12 hours, protected from light exposure, to allow DOPA polymerization. These samples were referred to as PE-Dopa. After this treatment, the PE-Dopa samples were washed with ultrapure water and dried in an oven at 40 °C. The chitosan-based suspension was then deposited by pipetting 350 μL onto the PE-Dopa surface and dried in an oven at 40 °C for 24 hours to produce the PE-Coated surface.

2.3 Morphology analysis

The samples' macro morphologies were examined by visual inspections recorded with a Canon EOS RebelT6 (Canon, Taipei, Taiwan). The sample's micro morphologies were analyzed by scanning electron microscopy (SEM) and profilometry. For SEM analysis, the specimens were placed on a tape and coated with gold for 3 minutes. The images were taken with a TESCAN VEGA3 microscope (TESCAN, Brno, Czech Republic), operating at an accelerating voltage between 10 and 15 kV with a working distance of 7–8 mm. Images were captured at a magnification of 1000×.

Surface roughness was assessed by profilometry measurements on a 1 mm² scan area. Images were acquired using a Bruker Dektak XT Profilometer (Billerica, MA, USA) with a tip radius of 12.5 μm and a stylus force of 3 mg.

2.4 Surface characterization

Surface characterization was carried out using X-ray Photoelectron Spectroscopy (XPS), and contact angle, as described elsewhere.[22,23] Briefly, XPS analyses were carried out using Physical Electronics PHI 5600-ci equipment (Chanhassen, MN, USA). A standard aluminum X-ray source (1486.6 eV) was used to record survey spectra with charge compensation, while high-resolution spectra were acquired using a standard magnesium X-ray source without neutralization. The detection was set at an angle of 45° concerning the surface normal, and the analyzed area was 0.5 mm². The experiments were performed for three different samples, which were measured three times in different positions to assess the homogeneity of the chemical composition. The curve fitting procedures for C 1s were performed employing a least-squares Gaussian–Lorentzian peak fitting procedure, after Shirley background subtraction. The C 1s peaks were set at 285 eV (C–C and C–H) as reference.

Static contact angle measurements were obtained using an OCA11 (DataPhysics, Filderstadt, Germany). Analyses were

performed at room temperature, with 3 μL droplets of ultrapure water deposited on five different areas per sample, and on three different samples.

2.5 Adhesion strength by (pull-off test)

The PE-Coated samples were subjected to a series of aging periods in PBS 1× solution, with durations of 1, 7, 14, 21, 28, and 35 days, respectively. After each aging period, the samples were dried at 35 °C in an oven and evaluated through a pull-off test. Additionally, a non-aged sample was used as a control. The test was executed according to the ISO 4624:2016 (ref. 24) standard with adaptations using an HSensor Mechanical Tester equipped with a 5 N load cell (HSensor, Maringá, Brazil), consisting of a sample support made of polylactic acid and a 1 cm² square flat indenter made of 304 stainless steel.

Firstly, PE-Coated samples of 2.25 cm² were fixed onto the sample support using a thin layer of super glue. Afterwards, the sample was fixed to the indenter using two layers of super glue: one on the top the sample, and another on the base of the indenter. The indenter was then placed in contact with the PE-Coated and allowed to dry for approximately 2 minutes. A force was applied upwards using a 5 N load cell at a speed of 0.08 mm s^{-1}, with a maximum duration of approximately 1.5 minutes. The adhesion force was calculated using the following equation:

$$\sigma = \frac{F}{A} \tag{1}$$

where σ is the adhesion strength [kPa], F is the adhesion force measured by the equipment [N], and A is the area of the indenter (1 cm²). The test was performed with five replicates for each condition.

2.6 Antibiotic release over time

The release of the antibiotic moxifloxacin over time was analyzed for both the chitosan-based film and the PE-Coated, and the obtained results were compared. The films were cut in 1.5 × 1.5 cm, the same size of PE-Coated to produce similar amount of material for comparison. To mimic physiological conditions, PBS 1× was used as the release medium at 37 °C under stirring at 150 rpm. Initially, 2 mL of PBS was added to each vial, and the medium was collected at intervals of 0 h, 1 h, 4 h, 24 h, 3 days, 7 days, and then every 7 days until the antibiotic was no longer detectable. After each sampling, fresh PBS was added. The collected samples were stored at −20 °C for later quantification by high-performance liquid chromatography (HPLC/UV Model 20-S, Shimadzu, Kyoto, Japan), as described elsewhere.[19,25] Limit of quantification was 0.5 μg mL^{-1} and limit of detection was 0.1 μg mL^{-1}. These experiments were performed in triplicate.

2.7 Antibacterial assays

2.7.1 Bacteria stock preparation. Eight bacterial strains commonly associated with biomaterial-associated infections were selected for this study: *Escherichia coli*, *Enterococcus faecalis*, *Staphylococcus aureus*, *Staphylococcus epidermidis*, methicillin-resistant *Staphylococcus aureus* (MRSA),

Pseudomonas aeruginosa, *Salmonella typhimurium*, and *Klebsiella pneumoniae*.[11] All stock bacteria were cultivated, maintained, and quantified as described previously.[19,26]

2.7.2 Antibacterial activity. Initially, the disk diffusion (Kirby–Bauer test),[27] was performed to compare the antimicrobial activity between the chitosan-based film and the PE-Coated with the same formulation. 100 μL of the $\sim 1 \times 10^8$ CFU per mL bacteria stock was spread with a Drigalski spatula onto 90 mm Petri dishes coated with fresh sterile Mueller–Hinton agar. Film and PE-Coated samples (cut into 6 mm diameter discs)[28] were sterilized with UV irradiation at 254 nm for 15 min on each side, and then placed on Petri dishes containing the bacteria. Paper disks impregnated with 10 μg moxifloxacin were used as the positive control, and uncoated clean PE discs were used as the negative control. The dishes were incubated at 37 °C for 24 h in an inverted position. Afterwards, the inhibition zones were measured using a digital pachymeter in three different positions. Experiments were carried out in at least one duplicate for each bacterium.

2.8 Biological test

2.8.1 Cell culture. The effects of the films on cell viability were analyzed using human dermal fibroblasts (HDFs). The cells were cultured in Dulbecco's modified Eagle's medium (D-MEM) with 10% foetal bovine serum (FBS), penicillin (100 U mL^{-1}), streptomycin (100 U mL^{-1}), at 37 °C, in a saturated atmosphere at 5% CO_2. Culture medium was changed every 48 hours until 85–90% of confluence was reached. Then, cells were enzymatically detached from the culture plates with 0.05% trypsin and reseeded at a ratio of 1 : 3 or used for experiments. Cells at passage 7 were used for the experiments.

2.8.2 Indirect cytotoxicity test. The indirect cytotoxicity test was performed following the ISO 10993-5:2009 procedure. Briefly, samples were cut into 1 cm^2 and sterilized with UV irradiation, undergoing 2 cycles of 15 minutes on each side. Afterwards, samples were immersed in 660 μl of D-MEM culture medium supplemented with 1% penicillin–streptomycin for 24 hours. After the 24 hours incubation, medium has been collected from samples and subsequently used for the viability test. Before putting them in contact with cells, extracted media have been supplemented with 10% fetal bovine serum (FBS). One day prior to contact with the extract, HDFs were seeded in the well of a 96 multi-well plate at a density of 20 000 cells per cm^2 and incubated at 37 °C and 5 vol% CO_2 for 24 hours in 100 μl per well of complete D-MEM medium. The day after, the medium was removed and 100 μl of the extracts were added to the well containing the cells and incubated for 24 hours. Normal complete D-MEM medium was used as a control (CTRL). The extracts were then removed and 100 μL of 1× solution of resazurin sodium salt in complete medium were added to the cells and incubated for 4 hours at 37 °C and 5 vol% CO_2. After the incubation, the solutions containing the now reduced resorufin product were collected and fluorescence intensity at a 545 nmex/590 nmem wavelength was measured with a SpectraMax i3x Multi-Mode Plate Reader (Molecular Devices, San Jose, California, USA). Fluorescence intensity is proportional to cell viability.

2.8.3 Hemolysis test. Whole human blood from a healthy donor has been collected in citrate-containing blood collection tubes. Each sample has been placed in a 15 mL tube and 10 mL of sterile PBS 1× have been added in each tube. PBS 1× has been used as a negative control and deionized H_2O as positive control. Then, the collected blood has been diluted in PBS 1× to a final ratio of 4 : 5 (4 parts of citrated blood and 5 parts of PBS 1×). After the incubation, 200 μL of diluted blood were added in each tube and carefully mixed by inverting each tube. After that, samples and controls were incubated at 37 °C for 1 h. All tubes have been carefully mixed by inversion after 30 minutes of incubation. At the end of the incubation, the tubes containing the samples and the controls underwent a centrifugation step at 800 g for 5 minutes. The supernatant was collected and 100 μL aliquots were placed in a 96-well plate. The absorbance (OD) at a wavelength of 540 nm has been recorded. The higher the absorbance, the higher the hemolysis. Finally, the hemolysis percentage has been calculated as follow:

$$\text{Hemolysis} = \frac{\text{OD samples} - \text{OD CTRL Pos}}{\text{OD CTRL Pos} - \text{OD CTRL Neg}} \times 100 \quad (2)$$

2.9 Statistical analysis

Statistical analyses were performed using Minitab® software (version 17, Minitab LLC, State College, PA, USA). All statistical comparisons were conducted using one-way ANOVA followed by Tukey's *post hoc* test. Data are presented as mean ± standard deviation (SD), and p-values < 0.05 were considered statistically significant.

3 Results and discussion

The morphology of uncoated polyethylene and PE-Coated was evaluated by optical and SEM microscopy. The images at 1000× magnification are shown in Fig. 1.

The macroscopic image of PE shows a white material (Fig. 1a), consistent with its medical grade purity. In contrast, the surface of PE activated with polydopamine displays a gray coloration (Fig. 1b), indicative of dopamine deposition and its concomitant polymerization.[29,30] The PE-Coated appears darker (Fig. 1c), providing a clear visual indication of the coating steps. This dark coloration is primarily attributed to the formation of colored complexes between tannic acid and iron. Additionally, the oxidation of tannic acid contributes to color change through its conversion into quinones, followed by polymerization and crosslinking with chitosan.[23,31,32]

SEM images reveal distinct surface features of PE at various stages of modification. The pristine PE surface exhibits aligned groove lines, characteristic of mechanical processing methods such as extrusion or compression molding (Fig. 1a). After polydopamine activation, the PE surface shows the presence of deposits (Fig. 1b), consistent with polydopamine deposition and oxidative polymerization. In contrast, the PE-Coated
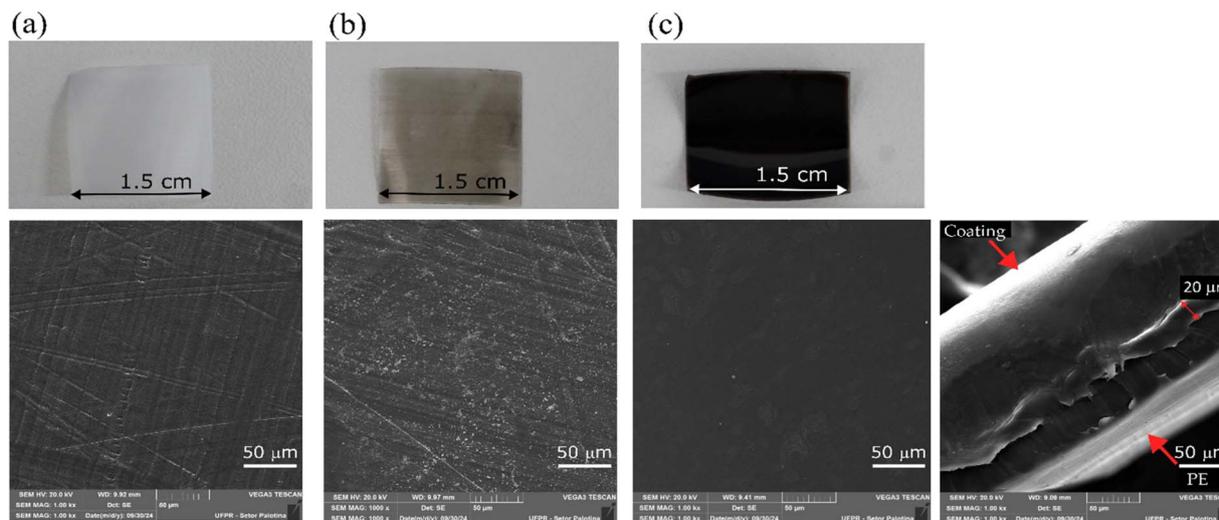
Fig. 1 Visual inspection and SEM images at $1000\times$ magnification of (a) uncoated PE, (b) PE–Dopa, and (c) PE-Coated, top view and side view.
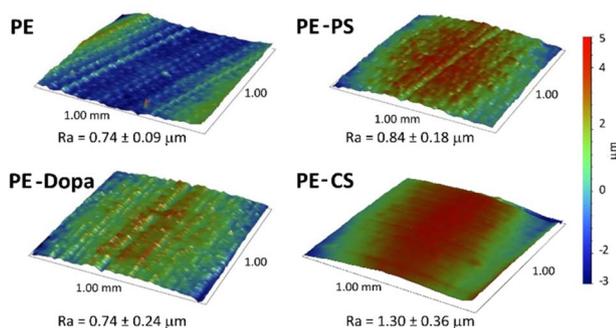

Fig. 2 Surface topography images and roughness values (R_a) for the PE, piranha-treated PE (PE–PS), dopamine-activated PE (PE–Dopa), and PE-Coated with the antibacterial chitosan-based formulation. All profilometry scans were acquired over the same area (1.0×1.0 mm^2) using the same scale bar. Measurements were performed with a stylus force of 3 mg.

displays a more homogeneous and smoother morphology (Fig. 1c and S1), suggesting effective surface coverage and modification. The average thickness of the film was 20 μm. For PE-Coated samples, the deposited amount of the coating material was controlled to obtain a comparable effective thickness. This ensured consistency across the samples and enabled comparison between the coatings and films throughout the study. To observe the topography of the coating, profilometry analysis was carried out, as shown in Fig. 2.

Surface roughness (R_a – roughness average) was measured to evaluate the impact of different treatments on PE surface texture. The uncoated PE surface exhibited a R_a of 0.74 ± 0.09 μm, with groove-like features that were also observed in SEM images. After piranha treatment, R_a increased to 0.84 ± 0.18 μm, likely due to the aggressive oxidation process, which roughened the surface. Subsequently, polydopamine treatment reduced R_a to 0.74 ± 0.20 μm, maybe due to dopamine deposition filling micro-roughness and smoothing out surface irregularities. Surprisingly, PE-Coated with the chitosan-based formulation displayed the highest R_a value, at 1.30 ± 0.36 μm.

To deepen the understanding of surface modifications, XPS was employed to determine the surface composition, along with chemical bonding states. The aim was to monitor each step of treatment to confirm the modification caused by the piranha treatment, polydopamine deposition, and finally PE-Coated. Data are shown in Table 1.

The XPS survey analysis revealed significant changes in the surface atomic composition across different PE treatments. The uncoated PE surface exhibited a high carbon content (95.4%), which decreased after chemical modifications, particularly in PE–PS and PE-Coated, likely due to oxidation and functional group incorporation.[33]

The oxygen content is high after piranha treatment (25%) compared with other chemical oxidizing agents from literature, such as dichromate (14.4%) and permanganate (17.9%)[34] and is comparable to the values reported of sulfonation of polyethylene with concentrated sulfuric acid under long exposures

Table 1 Surface atomic composition assessed by XPS survey analyses and contact angle

	% C	% O	% N	% S	Contact angle (°)
PE	95.4 ± 0.5	4.6 ± 0.5	0.0	0.0	89.0 ± 3.2
PE-PS	65.4 ± 6.8	25.0 ± 4.4	3.1 ± 0.7	5.7 ± 1.1	79.8 ± 4.5
PE-Dopa	72.5 ± 0.6	20.3 ± 0.7	7.2 ± 0.6	0.0	55.6 ± 3.2
PE-Coated	58.3 ± 0.9	31.0 ± 0.2	5.7 ± 0.6	3.3 ± 0.3	65.1 ± 2.3

(more than 1 h).[35] This high oxygen content evidences the incorporation of oxygenated groups and also sulfonic functionalities (–SO₃H). The simultaneous detection of sulfur (5.7%) corroborates this hypothesis. Such functionalities increase hydrophilicity, as confirmed by the reduced contact angle (79.8°), and create reactive anchoring sites that facilitate adhesion of the subsequent PDA and chitosan coatings. Oxygen content increased substantially in treated samples, with the highest value (31.0%) in PE-Coated, due to the presence of the chitosan-based formulation. The presence of nitrogen confirmed polydopamine deposition in PE-Dopa (7.2%) and chitosan-based formulation coating on PE-Coated,[36] unexpected nitrogen was observed on PE-PS sample (3.1%) maybe due to adsorption from air after treatment. Sulfur was also present in the PE-Coated (3.3%), since FeSO₄ is used in the chitosan-based coating.[19] Contact angle measurements highlighted increased hydrophilicity across all modified surfaces compared to PE, with PE-Dopa exhibiting the lowest value (55.6°) in agreement with polydopamine surface coating for other materials such as titanium and silica.[20] Overall, the treatments enhanced the PE surface wettability. The piranha treatment creates oxygen groups on the surface, which is important for the polydopamine deposition. The enhanced wettability and surface reactivity of PE-PS facilitate dopamine adsorption and subsequent oxidative polymerization, promoting the formation of a more uniform and adherent polydopamine interlayer. This interfacial activation step is therefore directly linked to the efficiency of the subsequent coating process.[37] The carbon-containing functional groups were identified by high-resolution C1 XPS spectra, as shown in Fig. 3.

The XPS analysis of C 1s spectra revealed distinct chemical modifications across the different PE treatments. Pristine PE exhibited a dominant peak at 285.0 eV (95.0%), corresponding to C–C/C–H bonds typical of unmodified polyethylene, with a minor shoulder at 286.5 eV (5.0%) possibly indicating impurities/defects originated from photooxidation.[38] Following piranha treatment, PE-PS retained a strong C–C/C–H signal at 285.0 eV (88.9%), but showed increased contributions at 286.5 eV (10.1%) and 288.9 eV (1.0%), reflecting oxidative functionalization and the formation of C–O and O=C–O species.[39] PE-Dopa exhibited a broadened spectral profile with peaks at 285.0 eV (63.0%), 286.5 eV (26.0%), and 288.5 eV (7.5%), indicating the incorporation of C–O, C–N, and carbonyl groups characteristic of polydopamine. Additionally, a π–π* satellite peak at 291.0 eV (3.5%) confirmed the presence of aromatic structures, typical of polydopamine.[40] PE-Coated displayed the most pronounced surface chemistry change, with a reduced C–C/C–H contribution at 285.0 eV (50.2%) and stronger signals at 286.5 eV (38.6%) and 288.5 eV (11.2%), consistent with the introduction of oxygenated and nitrogenous functional groups from chitosan.[22,23] These spectral differences highlight the chemical transformations induced by each treatment step.

Based on the surface chemistry, wettability, and topographical analyses presented above, the role of the polydopamine interlayer in enabling chitosan adhesion to polyethylene can be discussed. The polydopamine interlayer plays a central role in enabling the deposition of a chitosan coating onto the polyethylene substrate by acting as a chemically active interface. While polyethylene is intrinsically hydrophobic and chemically inert, the polydopamine layer introduces polar and reactive functional groups that promote interfacial compatibility with the chitosan matrix. This interlayer reduces the interfacial energy mismatch between PE and chitosan, facilitating uniform coating formation and improving resistance to delamination. A stable and well-anchored coating is essential to promote the moxifloxacin loading and release processes from a PE surface.[41]
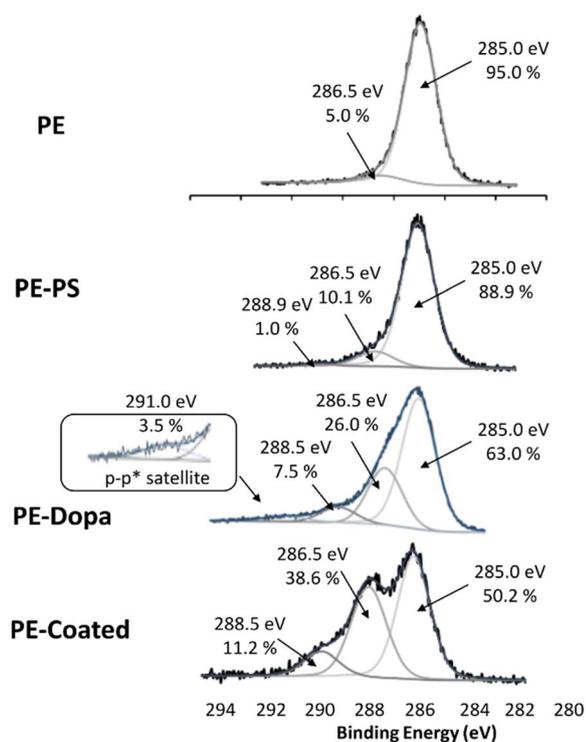

Fig. 3 High-resolution C 1s XPS spectra of PE samples before and after the coating process.

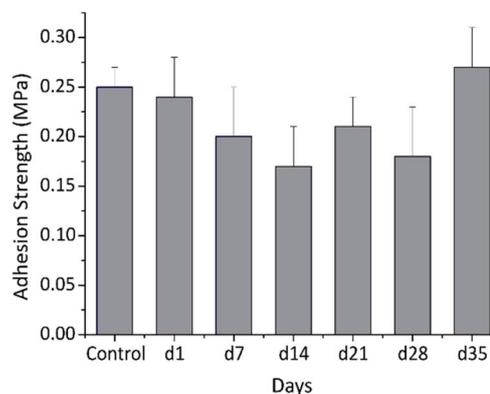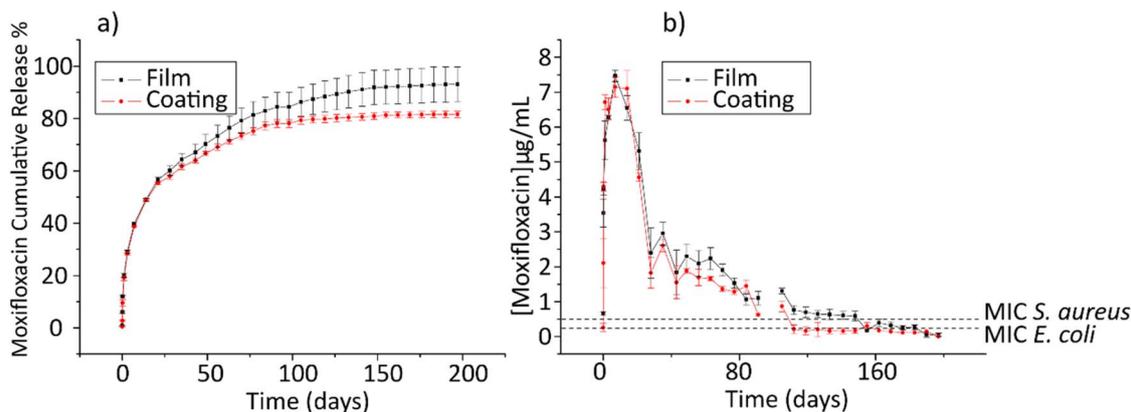**Fig. 4** Adhesion strength of PE-Coated aged in PBS, control is the freshly prepared samples.

Fig. 5 Release kinetics curves of moxifloxacin from chitosan–based films and coatings (a) cumulative antibiotic release and (b) concentration of moxifloxacin per time point. The dashed lines represent the MIC thresholds for antibacterial activity of moxifloxacin against *S. aureus* and *E. coli*. Studies carried out in PBS buffer at 37 °C, 150 rpm, pH 7.4. The figure shows the mean values ± SD measured at each time point.

At the molecular level, the stabilization of the chitosan layer on the polydopamine-modified surface is governed by multiple interaction. Polydopamine contains catechol and amine functionalities that can interact with chitosan through hydrogen bonding between hydroxyl and amine groups, as well as electrostatic and cation-π interactions. In addition, catechol groups can undergo to quinone species and create covalent bonding with chitosan amine groups *via* Schiff base formation or Michael-type addition, although such reactions are condition-dependent.[42] Together, these interactions can promote adherent and stable coatings, which was examined by the adhesion strength and its stability, determined by aging the material in a biologically relevant solution, namely PBS, as shown in Fig. 4.

The adhesion strength of the PE-Coated remained stable throughout the 35-days immersion period in PBS. The control sample was evaluated before immersion. Despite minor fluctuations, the coating consistently retained its adhesive properties during the aging process. The measured adhesion strength values (∼0.17–0.25 MPa) are comparable to those reported for ultrahigh molecular weight polyethylene (UHMWPE) coated with a chitosan/hydroxyapatite composite under similar pull-off test conditions.[43] Reports on the adhesion strength of chitosan-based coatings on PE are scarce in the literature, largely due to the inherently hydrophobic nature of PE and its poor interfacial bonding with polymeric matrices, which makes coating adhesion particularly challenging. Polydopamine has commonly been used as an intermediate layer to facilitate coating on low surface energy substrates.[44] For instance, on substrates with similarly low surface energy, such as polydimethylsiloxane, polydopamine-mediated surface functionalization has enabled the formation of chitosan-based coatings with adhesion strength values in the 0.02–0.04 MPa range.[22] In this study, coating attempts without this step failed.

To evaluate moxifloxacin release kinetics over time, a comparison was carried out between the film[19] and the PE-Coated as shown in Fig. 5. Both systems exhibited a two-phase cumulative release pattern with an initial burst during the first 10 days, followed by a sustained release phase, which is typical of chitosan-based systems.[21,45] Statistical analysis (ANOVA followed by Tukey's *post hoc* test), summarized in Table S1 (SI), confirmed that no significant differences were observed at early and intermediate time points, indicating comparable release kinetics for both systems up to 141 days. The film exhibited a higher cumulative release at long times (approximately 90%) compared to the coating, which plateaued at approximately 80%. This discrepancy reflects differences in the maximum attainable release rather than a change in the release mechanism and can be attributed to geometric constraints imposed by the substrate. In contrast, the free-standing film is fully exposed to the release medium. Nevertheless, the overall release behavior and kinetic profile of the two systems remain analogous.

The release of moxifloxacin from the film is primarily diffusion-dominated, as indicated by release exponent values n < 0.5 obtained from the Korsmeyer–Peppas model (Tables S2 and S3). However, the poor fitting of the Higuchi model over the complete release period suggests that the system does not follow ideal Fickian diffusion, likely due to deviations from the assumptions of matrix homogeneity and constant diffusivity. In this context, the superior performance of the Weibull model, evidenced by higher MSC and lower AIC values (Table S2), indicates a non-ideal diffusion process governed by matrix heterogeneity and time-dependent transport pathways rather than purely ideal diffusion kinetics. Given the close similarity between the kinetic parameters obtained for the film and the PE-Coated system, it is reasonable to assume that the same diffusion-dominated, non-ideal release mechanism governs drug release from the coating.[19,46,47] To further understand the drug release behavior, Fig. 5b presents the corresponding antibiotic concentrations at each time point. The initial burst release resulted in peak concentrations above 7 μg mL^{-1} for both systems. Importantly, concentrations remained above the minimum inhibitory concentration (MIC) for *S. aureus* (0.5 μg mL^{-1})[48] for 160 days in both the film and the coating, and consistently above the MIC for *E. coli* (0.25 μg mL^{-1})[48]

© 2026 The Author(s). Published by the Royal Society of Chemistry

Table 2 Disk diffusion results for the chitosan-based film and PE-Coated loaded with moxifloxacin against bacteria frequently found in biomaterial-associated infection (BAI)

Samples	Negative control[a] (mm)	Positive control[b] (mm)	PE-Coated (mm)	Film (mm)
Gram negative				
P. aeruginosa	0.0	30.5 ± 3.3^a	24.4 ± 0.5^b	19.0 ± 1.2^c
E. coli	0.0	27.8 ± 1.1^a	27.2 ± 0.8^a	24.1 ± 1.1^b
K. pneumoniae	0.0	$28.9 \pm 2.8^{a,b}$	$27.1 \pm 1.4^{a,b,c}$	$25.5 \pm 1.4^{b,c}$
S. typhimurium	0.0	32.4 ± 1.3^a	27.6 ± 1.6^b	27.8 ± 1.9^b
Gram positive				
E. faecalis	0.0	28.1 ± 1.2^a	20.7 ± 1.5^b	16.9 ± 1.6^c
S. aureus	0.0	29.3 ± 1.8^a	26.0 ± 1.4^b	23.7 ± 2.4^b
S. epidermidis	0.0	25.4 ± 3.6^a	23.3 ± 2.0^a	21.3 ± 1.5^a
MRSA	0.0	22.9 ± 0.9^a	16.3 ± 0.6^b	15.4 ± 0.6^b

[a] Disks of uncoated polyethylene. [b] Paper disc containing a 10 μg dose of moxifloxacin. Different superscript letters within the same row indicate statistically significant differences among the averages ($p < 0.05$). Groups sharing at least one letter are not significantly different.
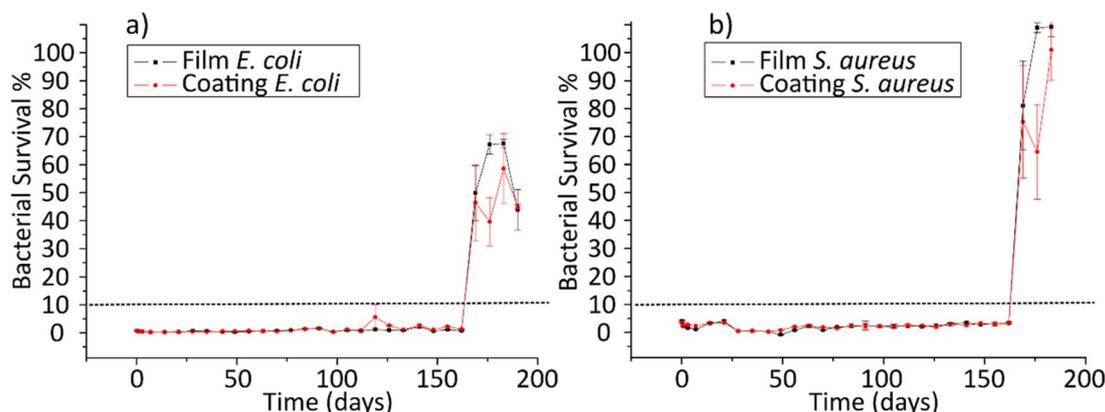
Fig. 6 Indirect antibacterial activity over time of chitosan-based film and PE-Coated against *E. coli* (a) and *S. aureus* (b). Studies carried out in Mueller–Hinton broth at room temperature, pH 7.4. The dashed line represents the threshold considered for contamination. The figure shows the mean values ± SD measured at each time point.

throughout the entire monitoring period, suggesting prolonged antibacterial effect.

The antibacterial effectiveness of the coating was initially assessed using a disk diffusion assay against clinically relevant bacterial strains and compared with the films (Table 2). Results of the uncoated PE disks (negative control) showed no inhibition zones, confirming the absence of intrinsic antibacterial properties. In contrast, the positive control (paper discs loaded with 10 μg of moxifloxacin) produced the largest inhibition zones, particularly against *S. typhimurium* (32.4 ± 1.3 mm), demonstrating the high efficacy of the free-form antibiotic, which is known to be a broad-spectrum antibacterial drug.[49,50] Both the chitosan-based film and PE-Coated exhibited substantial antibacterial activity, these findings confirm the antibacterial efficacy of PE-Coated and film against eight different pathogenic bacteria. In addition, a MRSA clinical isolate was included in the Gram-positive panel to expand antibacterial coverage.[51]

To gain additional insight about the antibacterial efficacy of the chitosan-based coatings and films, long-term bacterial

survival was monitored. While the disk diffusion assay demonstrated the antimicrobial activity in 24 h, this assay assessed how the sustained release of moxifloxacin affects bacterial inhibition over time. Fig. 6 presents the results of the
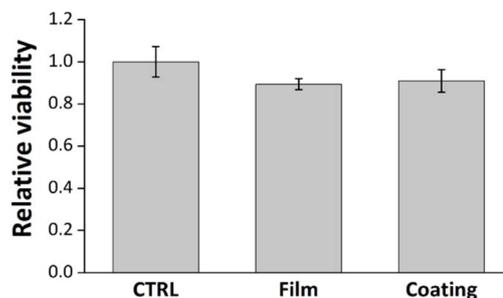
Fig. 7 Indirect cytotoxicity assay performed on human dermal fibroblasts. Cells have been incubated for 24 hours with extracts obtained from the following conditions: complete D-MEM medium (CTRL); chitosan-based film (Film) and PE-Coated (Coating).
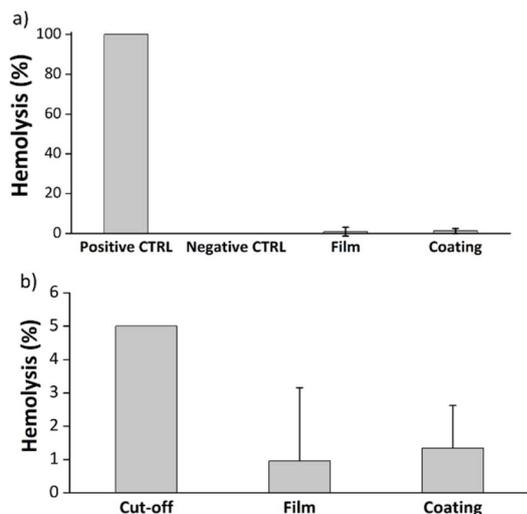
Fig. 8 Hemolysis test. (a) Shows the results of the hemolysis test performed on the different conditions compared to the positive control (CTRL Pos) and negative control (CTRL Neg) conditions. (b) Shows the differences between the tested samples and the 5% hemolytic cut-off.

indirect antibacterial assay, showing bacterial viability over time for *E. coli* and *S. aureus*. Both formulations maintained bacterial survival below 10% for approximately 160 days, which is the threshold established for this assay based on MIC determinations,[23,52] indicating effective inhibition of microbial

growth. After this period, a sharp increase in bacterial survival was observed, reflecting the depletion of moxifloxacin release. This threshold-type behaviour correlates with the concentration profiles shown in Fig. 5b, where moxifloxacin levels approach the MIC limits over time. Once the concentration falls below this critical threshold, a sharp increase in bacterial survival is observed. The antibacterial performance was comparable for both *E. coli* and *S. aureus*, confirming the broad-spectrum and long-lasting efficacy of the PE-Coated.

The results of the performed indirect cytotoxicity tests are presented in Fig. 7. As can be see, the developed antibacterial film, both in its original form or used as a coating for PE substrates, does not exert any cytotoxic effects towards human cells. In fact, no significant difference was noted towards the CTRL condition for both the tested conditions. The obtained results confirm the cytocompatibility of the film, showing how the film is not altered in a negative way by the grafting procedure. Both the film and the coating have also been tested in terms of their hemocompatibility. Results for the hemolysis tests are presented in Fig. 8.

As can be noted, none of the tested samples induced hemolysis. In fact, for a material to be considered hemolytic, it has to induce hemolysis at a percentage higher than 5% (Fig. 8b). Therefore, the tested conditions can be considered safe for blood contacting application.

The development of antibacterial coatings for PE has been widely explored, with studies primarily focusing on their ability to prevent biofilm formation and bacterial colonization, particularly in medical devices and packaging. However,

Table 3 Comparative analysis of chitosan-based coatings on polymers and metals: composition, maximum release time, and efficacy against tested bacteria

Author, year	Coating composition	Antibiotic/agent	Substrate	Release	Bacteria
This study	Chitosan, tannic acid, and iron	Moxifloxacin	Low-density polyethylene	160 days	*E. coli*, *S. aureus*, *S. epidermidis*, MRSA, *K. pneumoniae*, *P. aeruginosa*, *E. faecalis* and *S. typhimurium*
Asadi S. *et al.* 2022 (ref. 53)	Chitosan-coated titanium nanotubes	Ciprofloxacin	Titanium	1 day	*S. aureus*, *E. coli*
Srivastava M. G. *et al.* 2024 (ref. 54)	Chitosan, (3-glycidyloxipropyl) trimethoxy-silane	Chlorhexidine	Titanium	pH responsiveness, 12 days	*S. sobrinus*, *F. nucleatum*
Zhang A. *et al.* 2017 (ref. 55)	Carboxylated-chitosan, glutaraldehyde	Copper nanoparticle	Polyamide membrane	90 days	*E. coli*
Lin R. *et al.* 2022 (ref. 56)	Chitosan quaternary ammonium salt, collagen layer by layer	Chitosan quaternary ammonium	Titanium	90 days	*S. aureus*, *E. coli*, *E. faecalis*
Li X. *et al.* 2024 (ref. 57)	Chitosan quaternary ammonium salt layer by layer	Gentamicin	Titanium	14 days	MRSA and *E. coli*
Veloso F. D. *et al.* 2024 (ref. 22)	Chitosan, caffeic acid, and copper	Moxifloxacin	Silicon	21 days	*E. coli* and *S. aureus*
Lin C. *et al.* 2022 (ref. 58)	Catechol-modified chitosan microspheres	Triclosan and chlorhexidine	Silicon	40 days	*E. coli* and *S. aureus*
Zhou W. *et al.* 2018 (ref. 59)	Chitosan, heparin layer by layer	Tobramicin	Titanium	13 days	*E. coli* and *S. aureus*
Bile J. *et al.* 2016 (ref. 60)	PMMA microparticles	Phenylethyl alcohol	Polyethylene	90 days	Not tested

differently from this study, most research examines antibacterial effectiveness upon initial surface contact; long-term antibacterial activity over extended periods remains less frequently investigated. This study addresses that gap by demonstrating sustained, long-lasting antibacterial performance. Table 3 provides a comparative overview with selected examples from the literature. Table 3 shows that the chitosan–tannic acid–iron coating developed here provides prolonged antibacterial activity compared with other chitosan-based systems. This performance was achieved with a straightforward formulation and fabrication process, avoiding additional components such as nanoparticles or LBL assemblies. The coating remained active against Gram-positive and Gram-negative bacteria, including *E. coli*, *S. aureus*, *P. aeruginosa*, and *K. pneumoniae*, indicating its potential for long-term antimicrobial applications with practical advantages in processing and material use.

4   Conclusions

This study demonstrates a practical strategy for developing long-lasting antibacterial coatings on polyethylene (PE), a widely used material in medical devices. The coating consisted of a chitosan matrix crosslinked with tannic acid and iron and loading it with moxifloxacin, the coating achieved effective surface integration through a wet-chemistry approach involving piranha oxidation and polydopamine deposition. XPS analysis confirmed the presence of oxidized carbon species (C–O and O=C–O), after piranha treatment, and C–N after polydopamine deposition, which allowed the adhesion of the hydrophilic polymer onto the hydrophobic PE substrate. The resulting coating exhibited uniform surface and a roughness value of 1.3 ± 0.4 μm, with no signs of detachment or degradation after 35 days in PBS. Adhesion strength was maintained between 0.20 and 0.25 MPa during this period. Moxifloxacin release was sustained above the MIC for *S. aureus* and *E. coli* for over 160 days, which was confirmed by an indirect antibacterial assay. Importantly, the coating exhibited no toxicity towards dermal fibroblast human cells or hemolytic activity against red blood cell. Taken together, these findings support the potential of this coating for applications aimed at reducing biomaterial-associated infections through localized and prolonged antibiotic delivery.

Ethical statement

All blood donors gave their informed consent for inclusion before their participation in the study. The study was conducted in accordance with the Declaration of Helsinki, and the protocol was approved by the Ethics Committee of CR-CHU de Québec – Université Laval (2012-815, SCH11-09-091, SIRUL 95182).

Author contributions

H. J. W.: conceptualization, methodology, validation, formal analysis, investigation, visualization, supervision, writing – original draft, review & editing. N. F. S.: methodology, validation, formal analysis, investigation, visualization, writing – review & editing. P. C.: conceptualization, methodology, formal analysis, investigation, visualization, supervision, writing – review & editing. C. M. S.: methodology, validation, formal analysis, investigation, writing –review & editing. C. Z. B.: conceptualization, methodology, formal analysis, writing – review & editing. F. C.: conceptualization, methodology, formal analysis, investigation, visualization, writing – review & editing. D. M.: conceptualization, writing – review & editing, supervision, project administration and funding acquisition. All authors read and agreed with the final version.

Conflicts of interest

There are no conflicts to declare.

Data availability

Data for this article are available at https://doi.org/10.5281/zenodo.17751666 (accessed November 28, 2025).

Supplementary information (SI) is available. See DOI: https://doi.org/10.1039/d5ra09320a.

Acknowledgements

References

1 B. F. Finina and A. K. Mersha, *RSC Adv.*, 2024, **14**, 5290–5308, DOI: 10.1039/D3RA07884A.

2 A. S. Alzahrani, K. A. Alamry and M. A. Hussein, *RSC Adv.*, 2025, **15**, 32431–32463, DOI: 10.1039/D5RA04504E.

3 J. Sánchez-Bodón, M. Diaz-Galbarriatu, L. Pérez-Álvarez, I. Moreno-Benítez and J. L. Vilas-Vilela, *Coatings*, 2023, **13**, 1981, DOI: 10.3390/coatings13121981.

4 R. Bryaskova, N. Philipova, V. Bakov and N. Georgiev, *Appl. Sci.*, 2025, **15**, 1780, DOI: 10.3390/app15041780.

5 N. C. Paxton, M. C. Allenby, P. M. Lewis and M. A. Woodruff, *Eur. Polym. J.*, 2019, **118**, 412–428, DOI: 10.1016/j.eurpolymj.2019.05.037.

6 M. Hussain, R. A. Naqvi, N. Abbas, S. M. Khan, S. Nawaz, A. Hussain, N. Zahra and M. W. Khalid, *Polymers*, 2020, **12**(2), 323, DOI: 10.3390/polym12020323.

7 A. Gopanna, K. P. Rajan, S. P. Thomas and M. Chavali, in *Materials for Biomedical Engineering: Thermoset and Thermoplastic Polymers*, 2019.

8 K. N. Pandiyaraj, M. C. Ramkumar, A. Arun Kumar, P. V. A. Padmanabhan, M. Pichumani, A. Bendavid, P. Cools, N. De Geyter, R. Morent, V. Kumar, P. Gopinath, P. G. Su and R. R. Deshmukh, *Mater. Sci. Eng., C*, 2019, **94**, 150–160, DOI: 10.1016/J.MSEC.2018.08.062.

9 R. M. Donlan and J. W. Costerton, *Clin. Microbiol. Rev.*, 2002, **15**, 167–193, DOI: 10.1128/CMR.15.2.167-193.2002.

10 S. Sharma, J. Mohler, S. D. Mahajan, S. A. Schwartz, L. Bruggemann and R. Aalinkeel, *Microorganisms*, 2023, **11**, 1614, DOI: 10.3390/microorganisms11061614.

11 C. R. Arciola, D. Campoccia and L. Montanaro, *Nat. Rev. Microbiol.*, 2018, **16**, 397–409, DOI: 10.1038/s41579-018-0019-y.

12 R. C. Goy, D. de Britto and O. B. G. Assis, *Polímeros*, 2009, **19**, 241–247, DOI: 10.1590/S0104-14282009000300013.

13 X. Wang, M. Shan, S. Zhang, X. Chen, W. Liu, J. Chen and X. Liu, *Advanced Science*, 2021, **8**, 2104843, DOI: 10.1002/advs.202104843.

14 A. Popelka, I. Novák, M. Lehocký, I. Chodák, J. Sedliačik, M. Gajtanska, M. Sedliačiková, A. Vesel, I. Junkar, A. Kleinová, M. Špírková and F. Bílek, *Molecules*, 2012, **17**, 762–785, DOI: 10.3390/molecules17010762.

15 N. Harrasser, S. Jüssen, A. Obermeir, R. Kmeth, B. Stritzker, H. Gollwitzer and R. Burgkart, *Biomater. Res.*, 2016, **20**, 17, DOI: 10.1186/s40824-016-0062-6.

16 C. K. Nielsen, G. Subbiahdoss, G. Zeng, Z. Salmi, J. Kjems, T. Mygind, T. Snabe and R. L. Meyer, *J. Appl. Microbiol.*, 2018, **124**, 179–187, DOI: 10.1111/jam.13634.

17 S. H. Hsu, S. W. Whu, C. L. Tsai, Y. H. Wu, H. W. Chen and K. H. Hsieh, *J. Polym. Res.*, 2004, **11**, 141–147, DOI: 10.1023/B:JPOL.0000031080.70010.0b.

18 S. Rodrigues, M. Dionísio, C. R. López and A. Grenha, *J. Funct. Biomater.*, 2012, **3**(3), 615–641, DOI: 10.3390/jfb3030615.

19 N. F. Sczesny, H. J. Wiggers, C. Z. Bueno, P. Chevallier, F. Copes and D. Mantovani, *Antibiotics*, 2024, **13**, 1055, DOI: 10.3390/antibiotics13111055.

20 H. Lee, S. M. Dellatore, W. M. Miller and P. B. Messersmith, *Science*, 2007, **318**, 426–430, DOI: 10.1126/science.1147241.

21 I. T. Rampim, H. J. Wiggers, C. Z. Bueno, P. Chevallier, F. Copes and D. Mantovani, *Polymers*, 2025, **17**, 884, DOI: 10.3390/polym17070884.

22 F. Veloso, P. Chevallier, H. J. Wiggers, F. Copes, B. Drouin and D. Mantovani, *Coatings*, 2024, **14**, 291, DOI: 10.3390/coatings14030291.

23 P. Chevallier, H. J. Wiggers, F. Copes, C. Zorzi Bueno and D. Mantovani, *Nanomaterials*, 2023, **13**(1–18), 484, DOI: 10.3390/nano13030484.

24 I. O. for Standardization, *ISO 4624:2016 – Paints and Varnishes—Pull-Off Test for Adhesion*, Geneva, 2016.

25 U. S. Pharmacopeia, *USP–NF, United States Pharmacopeial Convention*, Rockville, MD, USA, 2020.

26 H. J. Wiggers, P. Chevallier, F. Copes, F. H. Simch, F. da Silva Veloso, G. M. Genevro and D. Mantovani, *Front. Bioeng. Biotechnol.*, 2022, **10**, 1–11, DOI: 10.3389/fbioe.2022.814162.

27 J. Hudzicki, Kirby-Bauer disk diffusion susceptibility test protocol, https://asm.org/protocols/kirby-bauer-disk-diffusion-susceptibility-test-pro, (accessed 3 September 2025).

28 NCCLS, *Methods for Dilution Antimicrobial Susceptibility Tests for Bacteria that Grow Aerobically-Sixth Edition*, Document M7-A6, Wayne, Pa, 2003.

29 A. L. de Souza, A. V. d. A. Oliveira, L. D. Ribeiro, A. R. F. e Moraes, M. Jesus, J. Santos, T. V. de Oliveira and N. d. F. F. Soares, *Polymers*, 2025, **17**, 345, DOI: 10.3390/polym17030345.

30 A. Telli and S. Arabaci, *Textil. Res. J.*, 2024, 00405175241274763, DOI: 10.1177/00405175241274763.

31 A. Espina, M. V. Cañamares, Z. Jurašeková and S. Sanchez-Cortes, *ACS Omega*, 2022, **7**, 27937–27949, DOI: 10.1021/acsomega.2c01679.

32 C. Chen, H. Yang, X. Yang and Q. Ma, *RSC Adv.*, 2022, **12**, 7689–7711, DOI: 10.1039/D1RA07657D.

33 F. S. F. dos Santos, J. F. B. Rodrigues, M. C. da Silva, M. E. V. Barreto, H. N. da Silva, S. M. de Lima Silva and M. V. L. Fook, *Molecules*, 2022, **28**, 74, DOI: 10.3390/molecules28010074.

34 D. Briggs, D. M. Brewis, R. H. Dahm and I. W. Fletcher, *Surf. Interface Anal.*, 2003, **35**, 156–167, DOI: 10.1002/sia.1515.

35 B. Xie, L. Hong, P. Chen and B. Zhu, *Polym. Bull.*, 2016, **73**, 891–908, DOI: 10.1007/s00289-015-1525-y.

36 H. Hemmatpour, O. De Luca, D. Crestani, M. C. A. Stuart, A. Lasorsa, P. C. A. van der Wel, K. Loos, T. Giousis, V. Haddadi-Asl and P. Rudolf, *Nat. Commun.*, 2023, **14**, 664, DOI: 10.1038/s41467-023-36303-8.

37 M. Benkocká, S. Lupínková, T. Knapová, K. Kolářová, J. Matoušek, P. Slepička, V. Švorčík and Z. Kolská, *Mater. Sci. Eng., C*, 2019, **96**, 479–486, DOI: 10.1016/j.msec.2018.11.066.

38 T. Di Giulio, G. E. De Benedetto, N. Ditaranto, C. Malitesta and E. Mazzotta, *Int. J. Mol. Sci.*, 2024, **25**, 5060, DOI: 10.3390/ijms25105060.

39 H. Bennet and O. G. J. Oliver, *J. Chem. Educ.*, 1993, **70**, A25, DOI: 10.1021/ed070pA25.

40 S. Rella, E. Mazzotta, A. Caroli, M. De Luca, C. Bucci and C. Malitesta, *Appl. Surf. Sci.*, 2018, **447**, 31–39, DOI: 10.1016/j.apsusc.2018.03.057.

41 H. M. Soylu, P. Chevallier, F. Copes, F. Ponti, G. Candiani, F. Yurt and D. Mantovani, *Front. Cell. Infect. Microbiol.*, 2021, **11**, 678081, DOI: 10.3389/fcimb.2021.678081.

42 S. Moulay, *Polym. Rev.*, 2014, **54**, 436–513, DOI: 10.1080/15583724.2014.881373.

43 A. Arizmendi-Morquecho, A. Chávez-Valdez, C. H. Navarro and K. J. Moreno, *Polym. Test.*, 2013, **32**, 32–37, DOI: 10.1016/j.polymertesting.2012.10.002.

44 W. Y. Quan, Z. Hu, H. Z. Liu, Q. Q. Ouyang, D. Y. Zhang, S. D. Li, P. W. Li and Z. M. Yang, *Molecules*, 2019, **24**(14), 2586, DOI: 10.3390/molecules24142586.

45 B. Özkahraman, E. Tamahkar, N. İdil, A. Kılıç Suloglu and I. Perçin, *Drug Dev. Res.*, 2021, **82**, 241–250, DOI: 10.1002/ddr.21747.

46 U. d. J. Martín-Camacho, N. Rodríguez-Barajas, J. A. Sánchez-Burgos and A. Pérez-Larios, *Int. J. Pharm.*, 2023, **639**, 123017, DOI: 10.1016/j.ijpharm.2023.123017.

47 N. A. Peppas and J. J. Sahlin, *Int. J. Pharm.*, 1989, **57**, 169–172, DOI: 10.1016/0378-5173(89)90306-2.

48 E. Matuschek, D. F. J. Brown and G. Kahlmeter, *Clin. Microbiol. Infection*, 2014, **20**, O255–O266, DOI: 10.1111/1469-0691.12373.

49 F. Van Bambeke, J.-M. Michot, J. Van Eldere and P. M. Tulkens, *Clin. Microbiol. Infection*, 2005, **11**, 256–280, DOI: 10.1111/j.1469-0691.2005.01131.x.

50 P. C. Appelbaum and P. A. Hunter, *Int. J. Antimicrob. Agents*, 2000, **16**, 5–15, DOI: 10.1016/S0924-8579(00)00192-8.

51 Y. Yang, Y. Liang, J. Chen, X. Duan and B. Guo, *Bioact. Mater.*, 2022, **8**, 341–354, DOI: 10.1016/j.bioactmat.2021.06.014.

52 J. M. Andrews, *J. Antimicrob. Chemother.*, 2002, **49**(6), 1049, DOI: 10.1093/jac/dkf083.

53 S. Asadi, B. Mortezagholi, A. Hadizadeh, V. Borisov, M. J. Ansari, H. Shaker Majdi, A. Nishonova, H. Adelnia, B. Farasati Far and C. Chaiyasut, *Pharmaceutics*, 2022, **14**, 1359, DOI: 10.3390/pharmaceutics14071359.

54 M. G. Srivastava, N. H. N. Kamarudin, M. K. Aktan, K. Zheng, N. Zayed, D. Yongabi, P. Wagner, W. Teughels, A. R. Boccaccini and A. Braem, *Pharmaceutics*, 2024, **16**, 377, DOI: 10.3390/pharmaceutics16030377.

55 A. Zhang, Y. Zhang, G. Pan, J. Xu, H. Yan and Y. Liu, *Sep. Purif. Technol.*, 2017, **176**, 164–172, DOI: 10.1016/j.seppur.2016.12.006.

56 R. Lin, Z. Wang, Z. Li and L. Gu, *Mater. Today Bio*, 2022, **15**, 100330, DOI: 10.1016/j.mtbio.2022.100330.

57 X. Li, F. Qi, J. Zhu, X. Niu, S. Yang and D.-G. Yu, *Mater. Today Commun.*, 2024, **41**, 110683, DOI: 10.1016/j.mtcomm.2024.110683.

58 C. Lin, Z. Huang, T. Wu, W. Xu, R. Zhao, X. Zhou and Z. Xu, *Pharm. Dev. Technol.*, 2022, **27**, 545–553, DOI: 10.1080/10837450.2022.2086571.

59 W. Zhou, Z. Jia, P. Xiong, J. Yan, M. Li, Y. Cheng and Y. Zheng, *Mater. Sci. Eng., C*, 2018, **90**, 693–705, DOI: 10.1016/j.msec.2018.04.069.

60 J. Bile, M.-A. Bolzinger, J.-P. Valour, H. Fessi and Y. Chevalier, *Drug Dev. Ind. Pharm.*, 2016, **42**, 818–824, DOI: 10.3109/03639045.2015.1081237.